Synthesis of large amounts of volatile element-bearing silicate glasses using a two-stage melting process

Paul Pangritz[a], Christian Renggli[a], Jasper Berndt[a], Arno Rohrbach[a], Stephan Klemme[a]

[a]Institut für Mineralogie, Corrensstrasse 24, Universität Münster, 48149 Münster, Germany

Paul Pangritz: Email: paul.pangritz@uni-muenster.de, ORCID: 0000-0002-5631-6982

Christian Renggli: Email: renggli@uni-muenster.de, ORCID: 0000-0001-8913-4176

Jasper Berndt: Email: jberndt@uni-muenster.de

Arno Rohrbach: Email: arno.rohrbach@uni-muenster.de

Stephan Klemme: Email: stephan.klemme@uni-muenster.de ORCID: 0000-0001-7859-9779

Keywords: silicate melts, glass synthesis, volatiles, volatile bearing glass, evaporation

Abstract:

The evaporation of volatile and moderately volatile elements from silicate glasses is an important topic in geosciences, environmental, and materials science. Glasses that contain volatile elements are used in a wide range of experimental studies, but the synthesis of volatile bearing glasses at high temperatures as well as the choice of starting materials is challenging. Here we present a new method for the synthesis of 15-20g moderately volatile and volatile element bearing boron-aluminosilicate glasses using a two-stage melting process. Results show that the glasses contain between 7000 and 10000 µg/g Zn, Cu, or Te and ~3000 µg/g S. In-situ analyses with scanning electron microscope (SEM) and electron microprobe analysis (EPMA) confirm that all glasses are homogenous for major and trace elements within the analytical uncertainties.

Introduction:

Silicate glasses and melts are ubiquitous phases, both in geological systems on Earth and other planetary bodies [1]. Natural silicate glasses contain volatile elements (e.g., S, Cl, H) which play a key role in several geological processes such as element transfer in subduction zones, volcanic degassing, contamination of atmospheres, or ore-forming processes [2]. The behavior of volatile and moderately volatile elements, such as Cu, and Zn during evaporation from silicate melts is an active field of research [3–9] but neither the geochemical character (i.e., siderophile, lithophile,

chalcophile, or atmophile) of these elements nor the behavior of these elements during evaporation as a function of temperature and oxygen fugacity is well understood. Additionally, complexing elements such as S or Cl may affect the volatility of these metals [10].

Furthermore, silicate glasses are commonly used as starting materials in experimental geosciences or reference materials for microanalytical methods [11–13]. However, as silicate glasses are usually prepared at high temperatures, most glasses were prepared in simplified chemical compositions and hence did not contain volatile elements. However, as natural silicate melts and glasses can contain several weight percent of volatile and moderately volatile elements, a novel method for the synthesis of large amounts of volatile element bearing boron-aluminosilicate glasses is clearly needed. Furthermore, most reference materials that are employed for microanalytical studies in the geosciences, environmental, and materials sciences are glasses that are either free of volatile elements or seriously zoned in volatile elements [14,15]. New homogeneous glasses with known volatile element concentrations would be beneficial to a large community of scientists that are concerned with microanalysis of geological materials.

The aim of this study is to identify a method with which large amounts (~15-20g) of homogenous and undegassed volatile-bearing glasses can be prepared. The glasses may serve as reference materials for microanalysis, and as starting materials for evaporation- and degassing experiments. Hence we set out to prepare large amounts of volatile-rich silicate

glasses using several starting material compositions with varying experimental strategies. The synthesized glasses contain Cu, Zn, Te, and S, and were characterized for homogeneity and composition using different analytical techniques.

Experimental Strategy

Volatile-rich starting material glasses can be synthesized at high pressures, e.g., using internally heated pressure vessels [16], or the piston-cylinder apparatus [9,17]. However, high-pressure synthesis of glasses yields only small amounts (at best in the order of a few 100 mg) of undegassed and homogenous glass, which is probably not enough material for a systematic series of evaporation experiments or as reference material for microanalysis.

Hence we decided to explore the possibility to prepare volatile-element bearing glasses at atmospheric pressures in conventional noble metal crucibles. However, initial tests in haplobasaltic melt compositions yielded glasses that were heavily zoned in the volatile elements, with almost complete degassed glass zones at the top of the crucible and less degassed glasses towards the bottom of the crucible (Figure. 1a below). This observed zonation of the glass in the crucible increases with run duration, temperature, and decreasing viscosity of the melt. Hence we set out to identify suitable melt compositions, run durations, and temperatures to prevent evaporative loss of volatile elements from the glass. Our ultimate goal was to prepare

a volatile-element bearing glass in the crucible which has only a thin degassed layer on top and a large reservoir of undegassed glass below (Figure 1b).

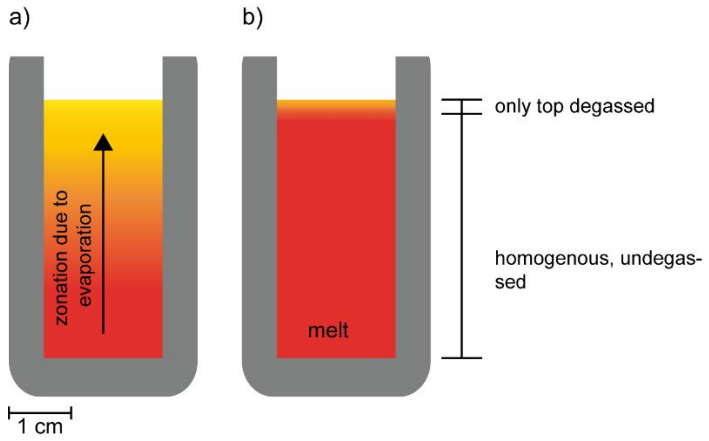

Figure 1. (a) Initial experiments in haplobasaltic compositions resulted in a strongly zoned glass, with low concentrations of the volatile elements at the top of the crucible (yellow area) and higher concentrations of volatile elements towards the bottom of the crucible. (b) An ideal experiment: the glass contains high concentrations of volatile elements, only a thin layer of glass at the very top of the crucible has lost elements due to evaporation but most of the glass is undegassed and homogeneous.

Experimental and Analytical Methods:

Starting materials

Initially, we prepared glasses in a haplobasaltic composition at the anorthite ($CaAl_2Si_2O_8$) – diopside ($CaMg_2Si_2O_6$) eutectic at $An_{36}Di_{64}$ [18]. Starting material mixtures were prepared using reagent-grade MgO, Al_2O_3, and SiO_2 (Sigma Aldrich, GmbH, Germany), and $CaCO_3$ (Alfa Aesar GmbH, Germany). To release any adsorbed water or hydroxides, MgO was previously fired at 1000˚C for more than 12 hours and subsequently stored at 110˚C in a drying cabinet. As initial tests showed that the liquidus temperature of 1275˚C of this composition in the system CaO-MgO-Al_2O_3-SiO_2 was too high to prevent evaporative loss of volatile elements, we added B (using boric acid (H_3BO_3) (ABCR-GmbH, Germany) to further decrease the liquidus of the system.

Glass synthesis

We used a Linn HighTherm VMK1800 (Linn GmbH, Germany) box furnace to prepare our glasses. Temperatures within the furnace are monitored and controlled by a $Pt_{70}Rh_{30}$ – $Pt_{94}Rh_6$ (type B) thermocouple connected to a Eurotherm 2416 (Schneider Electric Systems, Germany) controller. The furnace is pre-heated to the given temperature at least 30 minutes before the

experiments to ensure it is thermally equilibrated and that temperature variations within the furnace are negligible.

Starting material compositions (Table 1) were homogenized using an agate mortar with ethanol for one hour and stored in a drying cabinet (50˚C) to evaporate any residual ethanol. Because Ca was added to the mix as $CaCO_3$ and B_2O_3 as H_3BO_3, the starting material mixture was fired at 1000˚C for 3 hours to decarbonate the $CaCO_3$ and to convert the H_3BO_3 to B_2O_3 [19]. The resulting mixture was reground under ethanol to a fine powder, and the resulting mixture was vitrified in a Pt crucible (this is the "stage 1" of our glass preparation procedure, see flowchart (Figure 2) below) at 1200˚C for 30 minutes, and subsequently quenched by tipping the bottom of the crucible into the water bath and fully dropping it in after a few seconds.

Table 1. starting material compositions (in g)

	Sulfur-containing			Sulfur-free	
Starting material	**PPG07**	**PPG09**	**PPG11.2**	**CRG01**	**PPG11**
$CaCO_3$	5.5380	5.5380	5.7409	5.9264	5.9318
MgO	1.4936	1.4934	1.5481	1.5286	1.5279
Al_2O_3	2.1253	2.1254	2.2019	2.1734	2.1745
SiO_2	6.9591	6.9590	7.2113	7.1177	7.1170
H_3BO_3	3.1826	3.1826	3.2991	3.2551	3.2552
$CaSO_4$	0.3152	0.7008	0.3381	-	-
TeO_2	-	-	-	0.1538	-
CuO	-	0.3152	-	-	-
Cu_2O	-	-	-	-	-
ZnO	-	-	0.2023	-	0.272

The colorless “stage 1” glass then was crushed and ground to a fine powder using the agate mortar and ethanol again for one hour. The glass powder was doped with the respective element (as oxides for Cu, Te, and Zn and $CaSO_4$ for S). Note that the choice of the phase as which the volatile element is added to the starting material, is enormously important for the glass synthesis: Initial experiments showed that the glasses that were prepared with compounds such as elemental S, lost all S during the glass-making procedure and we speculate that the evaporative loss of S probably happened before the actual glass had formed. A much better choice is sulfate as the S-source in the starting material, and our results show that the glasses are not degassed in S. Similarly, the use of metal oxides (e.g. ZnO) is better than Zn from standard solutions or metallic Zn. Trace elements and “stage 1” glass were then homogenized for at least one hour in the agate mortar with ethanol and dried under red light.

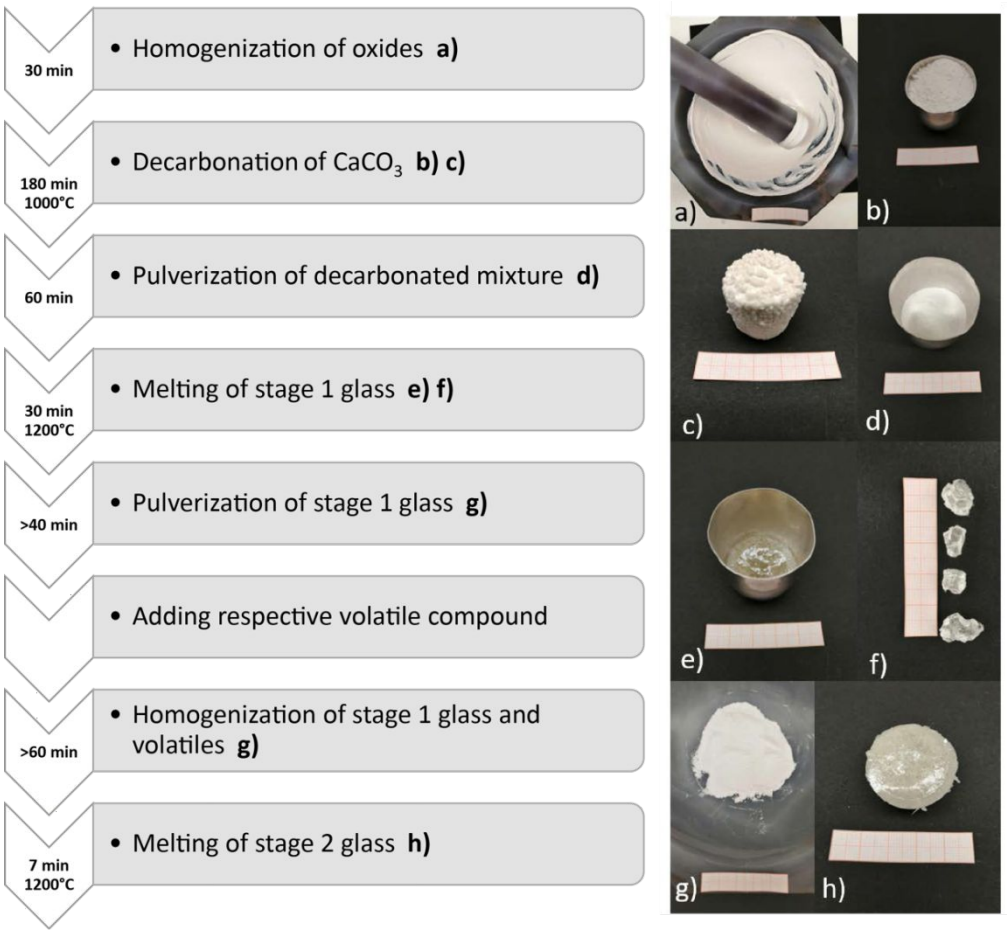

Figure 2. Flowchart showing different steps for glass synthesis with runtimes, temperatures (left), and corresponding photos of the synthesis (right). To ensure a homogenous starting material, pulverization of the decarbonated and partly sintered mixture (c), as well as the homogenization of volatile compounds with the first stage glass (e-g) is extremely important for a successful synthesis.

Starting compositions were placed into a Pt crucible under slight compression with a pestle to minimize pore space in the starting material and consequently gas bubble formation during vitrification. The mixture is subsequently vitrified at 1200˚C for 7 minutes and quenched in

cold water again. We found that 7 minutes runtime proved to be the best compromise to allow for homogenization of the melt and to prevent volatile element loss due to evaporation. The stage 2 glass, in contrast to the stage 1 glass, appears opaque and white-colored by the fact that the low melting duration of the final vitrification is too short to let all leftover air escape through the melt.

Analytical methods:

The glasses were mounted in epoxy resin, polished, carbon-coated, and first examined using a JEOL 6510 LA scanning electron microscope (SEM). Major element concentrations of all phases were determined with a 5-spectrometer JEOL JXA 8530F electron microprobe analyzer (EMPA) at the Institute für Mineralogie at the Westfälische Wilhelms-Universität Münster (WWU). All glasses were measured with 15kV acceleration voltage, a beam current of 60 nA, and beamsize of 10µm. Counting times were 120 s on peak and 60 s on the background for B, S, Cu, Zn, and Te. All other elements were measured with 20 s on the peak and 10 s on the background. A set of well-characterized synthetic and natural reference materials were used for standardization. Precision and accuracy were monitored by measuring secondary standards that were not used for calibration.

Table 2. EMPA measurement conditions and reference materials

Element	Diff. Crystal	Peak Pos. nm	Bkg. Position. L mm	Bkg. Position. U mm	Ref. material
B	LDE2	195.807	25	25	Ast_BN
Al	TAP	90.868	5	5	H_DistheneR8
Mg	TAP	107.731	2.8	4	U_OlivineSanCarlos
Si	PETJ	228.169	3	2	U_Hypersthene
Ca	PETJ	107.379	5.5	4.5	H_DiopsideST48
Cu	LIFH	107.013	1.5	2	H_Kupferkies
Zn	LIFH	99.685	3	3	Ast_Willemite
Te	LIFH	105.04	3.5	7.5	Ast_Te
Te	PETL	105.548	3.5	7.5	Ast_Te
S	PETL	172.073	3.5	3	Ast_Pyrite

Tellurium measurements were performed on two spectrometer crystals to increase counts per second.

Results:

Textural observations

The S-, Zn-, and Te-bearing glasses were white or slightly cloudy, whereas the Cu-bearing glass had deep blue color, probably caused by Cu^{2+}. Initial characterization of the glasses with SEM shows that the cloudy nature of some glasses is due to small gas bubbles, which were homogeneously distributed within the glass (Figure 3). However, we find that the bubbles are formed from air within the starting material powder due to incomplete sintering, and not from evaporating volatile compounds during the melting process. This interpretation is supported by the fact, that the glass composition does not change in the vicinity of the bubbles for any element. We observed no leftover oxide grains or other impurities within the bubbles or the glass. The Te-bearing glass (CRG01) is less cloudy due to fewer gas bubbles. The bubble formation was minimized by compression of the powder in the crucible before melting. The CuS glass (PPG09) was frothy but homogenous because of the decomposition of 2CuO into Cu_2O and $½O_2$

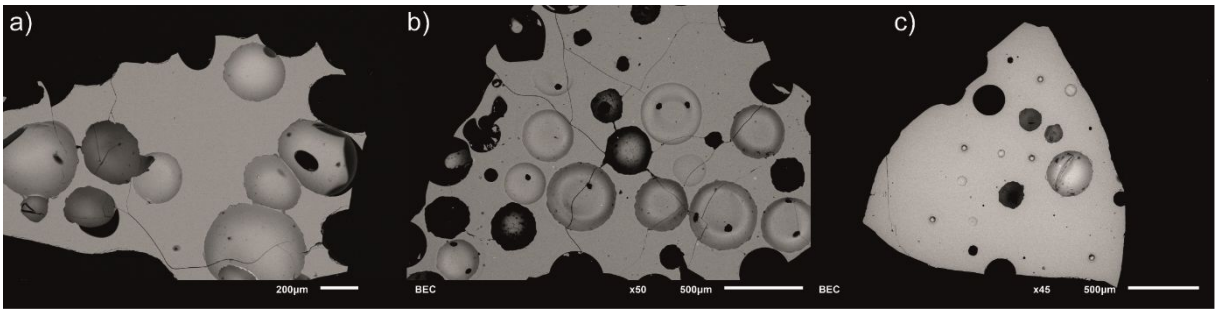

Figure 3. Backscattered electron images (BSE) of PPG09 (a), PPG07 (b), and CRG01 (c) glasses. Observed bubbles are a relic of leftover air in the starting material. There is no change in composition closer to bubbles. The difference in shape and size is explained by different depths of the bubbles relative to the polishing surface. Smaller particles inside the bubbles are not condensed volatile element grains, but particles of the polishing pastes that were used during sample preparation. Small white circles in the CRG01 glass (c) show ablation craters from Laser-ablation ICP-MS measurements.

Major and minor element analysis

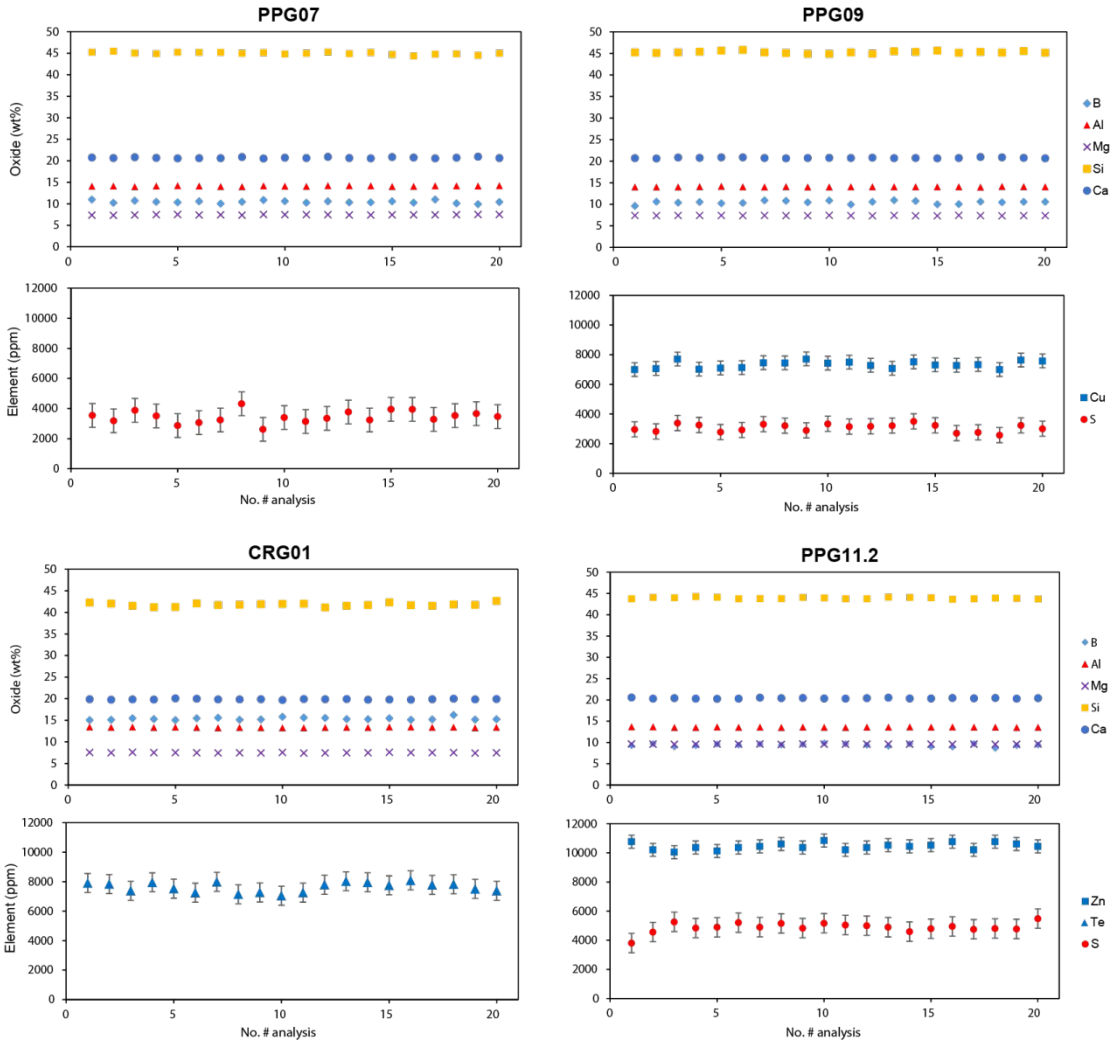

Figure 4. Major and minor element composition of synthesized boron-aluminosilicate glasses (EMPA analyses). The x-axis shows randomly picked glass analyses from different crucible parts. Error bars represent two times the standard deviation. Major (Si, Ca, Al, B, and Mg) and minor (S, Cu, Te, and Zn) elements are evenly distributed in the samples within the errors. The error bars of the major element data are smaller than the symbols.

Figure. 4 shows element abundances in the glasses. Major and minor elements are homogeneously distributed within the glass. The top and bottom parts of the glasses in the crucibles were analyzed separately (see Figure 5) to assure that no evaporation occurred during the melting process. Both, upper and lower crucible parts show the same elemental abundances within the analytical error for all elements measured. Slightly varying concentrations, (e.g. S concentrations in the bottom right diagram) are probably caused by not fully homogenized starting mixtures.

Table 3. EPMA measurements

	CRG01		PPG07		PPG09		PPG11.2	
	av.	**σ**	**av.**	**σ**	**av.**	**σ**	**av.**	**σ**
SiO_2	41.78	0.38	44.97	0.263	45.28	0.24	43.89	0.167
Al_2O_3	13.34	0.069	14.10	0.077	14.06	0.070	13.58	0.048
MgO	7.51	0.048	7.44	0.052	7.40	0.025	9.61	0.030
CaO	19.89	0.084	20.71	0.123	20.76	0.080	20.38	0.088
B_2O_3	15.38	0.28	10.45	0.28	10.48	0.36	9.36	0.31
TeO_2	0.95	0.04	-	-	-	-	-	-
SO_3	-	-	0.86	0.098	0.77	0.062	1.22	0.08
ZnO	-	-	-	-	-	-	1.30	0.028
CuO	-	-	-	-	0.92	0.029	-	-
Sum	**98.85**		**98.53**		**99.66**		**99.33**	

Chemical analyses of the glasses were performed using EPMA, and average values (av) are given together with analytical uncertainties (**σ)** as the standard deviation of all measurements.

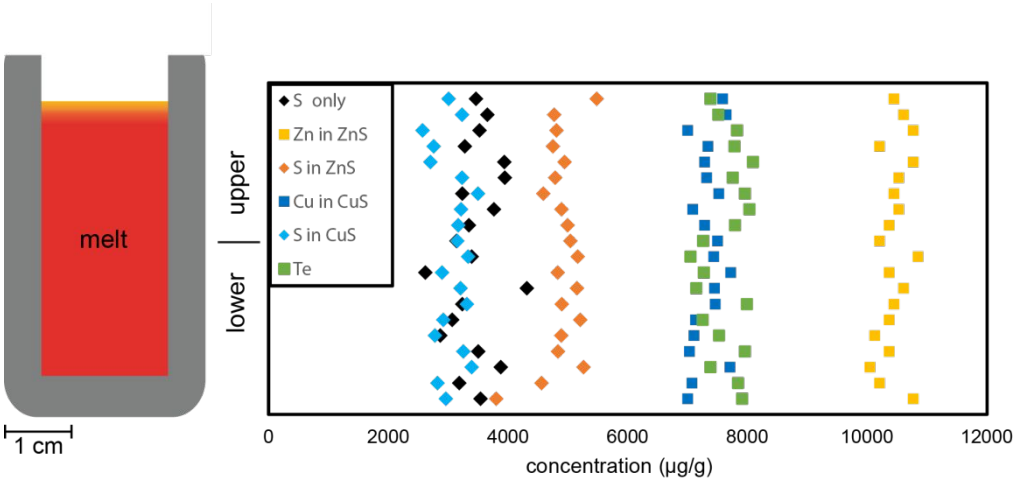

Figure 5. Vertical profiles through the ca. 6 cm high Pt crucibles. EMPA analysis shows no evaporation of elements in the upper or uppermost parts of the crucible.

Discussion

We find that the successful synthesis of large amounts (i.e. several grams) of volatile-bearing silicate glasses critically depends on the choice of volatile element compound in the starting material. The volatile-element compound needs to be stable at high temperatures (have a high melting point and high solubility in silicate melts) but it must also dissolve rapidly in the silicate melt and diffuse quickly within the melt, as our results show that short (7min) melting duration for the final glass is optimal. Our results show that the starting material compounds TeO_2, CuO/Cu_2O, $CaSO_4$, and ZnO give the best results. Previous runs where elemental Sulfur, SeO_2, and Se standard solution (such as those used in ICP-MS analyses) were used in the starting material led to complete degassing of these elements in the glass. Note that the major element composition, melt viscosity and run temperatures were kept constant in all these runs so that the degassing of these starting materials is only ascribed to low decomposition temperatures and/or instability of the starting material compounds at high temperatures. Alternatively to the use of sulfate, our results show that S may be added as a sulfide, but this requires glass synthesis under highly reducing conditions below the iron-wustite buffer (IW), where S has a high solubility in silicate melts [20]. Similarly, Se and Te-bearing glasses may be prepared at reducing conditions <IW, using selenide and telluride compounds.

Conclusions

We present a new two-stage method for the synthesis of large amounts of homogenous, unzoned glasses with high amounts of volatile elements such as S, Cu, Te, and Zn. These glasses may be used as starting materials for evaporation experiments, or reference materials for microanalyses with EMPA or LA-ICP-MS.

AUTHOR INFORMATION

Corresponding Author

Paul Pangritz – Institut für Mineralogie, Westfälische Wilhelms-Universität Münster, Germany. Email: paul.pangritz@uni-muenster.de

Paul Pangritz – Institut für Mineralogie, Westfälische Wilhelms-Universität Münster, Germany. Email: paul.pangritz@uni-muenster.de

Christian Renggli - Institut für Mineralogie, Westfälische Wilhelms-Universität Münster, Germany. Email: renggli@uni-muenster.de, Phone: +49 251 83-33452

Jasper Berndt - Institut für Mineralogie, Westfälische Wilhelms-Universität Münster, Germany. Email: jberndt@uni-muenster.de, Phone: +49 251 83-33049

Arno Rohrbach - Institut für Mineralogie, Westfälische Wilhelms-Universität Münster, Germany. Email: arno.rohrbach@uni-muenster.de, Phone: +49 251 83-36138

Stephan Klemme - Institut für Mineralogie, Westfälische Wilhelms-Universität Münster, Germany. Email: stephan.klemme@uni-muenster.de, Phone: +49 251 83 33047

Author Contributions

All authors have given approval to the final version of the manuscript.

Funding Sources

We acknowledge funding by the Deutsche Forschungsgemeinschaft (DFG)—Project-D 263649064—SFB TRR-170. This is SFB TRR 170 publication no. Xxx. CR is funded by the Deutsche Forschungsgemeinschaft (DFG, German Research Foundation) – project 442083018.

ACKNOWLEDGMENT

Our thanks go to Beate Schmitte for her superb support during EPMA, Maik Trogisch for his excellent sample preparation, Peter Weitkamp, Christopher Fritzsche in the precision engineering workshops, and Ludger Buxtrup, Samuel Flunkert, and Andrew Hardes for support in all things electronics.

Table.4: Electron microprobe analyses of sample PPG07

No.	B_2O_3	Al_2O_3	MgO	SiO_2	CaO	SO_3	ZnO	CuO	TeO_2	Total
1	10.86	14.16	7.51	45.12	20.53	0.65	-	-	-	99.24
2	10.34	14.19	7.50	45.22	20.55	0.72	-	-	-	98.57
3	10.57	14.12	7.39	45.18	20.62	0.77	-	-	-	98.92
4	10.28	14.05	7.47	45.00	20.66	0.78	-	-	-	98.44
5	10.21	14.12	7.34	45.45	20.65	0.80	-	-	-	98.52
6	10.04	14.01	7.45	45.17	20.61	0.81	-	-	-	98.65
7	10.34	14.15	7.40	45.13	20.56	0.81	-	-	-	98.09
8	10.97	14.16	7.43	44.77	20.58	0.82	-	-	-	98.71
9	10.55	14.19	7.48	45.26	20.91	0.84	-	-	-	98.83
10	10.62	14.08	7.48	44.79	20.71	0.85	-	-	-	98.53
11	10.43	14.21	7.50	44.98	20.63	0.87	-	-	-	98.24
12	10.47	14.10	7.46	44.86	20.67	0.88	-	-	-	99.23
13	10.12	14.14	7.49	44.84	20.73	0.88	-	-	-	98.43
14	10.97	14.06	7.36	45.22	20.75	0.88	-	-	-	98.39
15	9.93	14.10	7.51	44.49	20.94	0.91	-	-	-	98.57
16	10.32	14.21	7.41	44.89	20.66	0.94	-	-	-	97.81
17	10.71	13.96	7.39	45.05	20.84	0.97	-	-	-	98.73
18	10.26	14.05	7.42	44.35	20.75	0.98	-	-	-	98.20
19	10.58	14.01	7.43	44.68	20.88	0.99	-	-	-	97.88
20	10.44	13.95	7.36	45.00	20.88	1.08	-	-	-	98.62
Mean	10.45	14.10	7.44	44.97	20.71	0.86				98.53
Std.	0.28	0.08	0.05	0.26	0.12	0.10				0.37

Table.5: Electron microprobe analyses of sample PPG11.2

No.	B_2O_3	Al_2O_3	MgO	SiO_2	CaO	SO_3	ZnO	CuO	TeO_2	Total
1	9.21	13.65	9.66	43.74	20.58	0.95	1.34	-	-	99.13
2	9.71	13.67	9.62	44.05	20.28	1.14	1.27	-	-	99.74
3	8.95	13.52	9.57	43.97	20.40	1.31	1.25	-	-	98.97
4	9.23	13.50	9.56	44.25	20.29	1.21	1.29	-	-	99.33
5	9.59	13.61	9.63	44.11	20.26	1.22	1.26	-	-	99.68
6	9.39	13.54	9.62	43.73	20.31	1.30	1.29	-	-	99.18
7	9.61	13.57	9.65	43.77	20.52	1.22	1.30	-	-	99.64
8	9.36	13.52	9.55	43.79	20.40	1.29	1.32	-	-	99.23
9	9.54	13.60	9.63	44.05	20.45	1.21	1.29	-	-	99.77
10	9.86	13.55	9.60	43.95	20.32	1.29	1.35	-	-	99.92
11	9.67	13.51	9.62	43.76	20.31	1.26	1.27	-	-	99.40
12	9.34	13.60	9.59	43.74	20.41	1.25	1.29	-	-	99.22
13	9.12	13.60	9.61	44.12	20.51	1.22	1.31	-	-	99.49
14	9.67	13.63	9.62	44.05	20.33	1.15	1.30	-	-	99.75
15	9.00	13.59	9.61	43.96	20.32	1.20	1.31	-	-	98.99
16	8.93	13.61	9.58	43.63	20.44	1.24	1.34	-	-	98.77
17	9.71	13.59	9.6	43.75	20.37	1.19	1.27	-	-	99.48
18	8.62	13.60	9.57	43.90	20.46	1.20	1.34	-	-	98.69
19	9.24	13.52	9.58	43.82	20.29	1.19	1.32	-	-	98.96
20	9.38	13.53	9.64	43.71	20.42	1.37	1.30	-	-	99.35
Mean	9.36	13.58	9.61	43.89	20.38	1.22	1.30	-	-	99.33
Std.	0.31	0.05	0.03	0.17	0.09	0.08	0.03	-	-	0.34

Table.6: Electron microprobe analyses of sample PPG09

No.	B_2O_3	Al_2O_3	MgO	SiO_2	CaO	SO_3	ZnO	CuO	TeO_2	Total
1	9.63	14.00	7.4	45.24	20.71	0.74	-	0.88	-	98.60
2	10.62	13.99	7.39	45.12	20.62	0.71	-	0.89	-	99.33
3	10.4	13.99	7.4	45.23	20.86	0.85	-	0.96	-	99.69
4	10.52	14.08	7.40	45.39	20.79	0.81	-	0.88	-	99.87
5	10.24	14.14	7.42	45.63	20.9	0.69	-	0.89	-	99.91
6	10.3	14.05	7.36	45.78	20.88	0.73	-	0.89	-	99.99
7	10.9	13.99	7.41	45.21	20.75	0.83	-	0.93	-	100.02
8	10.79	14.08	7.36	45.06	20.67	0.80	-	0.93	-	99.69
9	10.47	14.01	7.39	44.89	20.72	0.72	-	0.97	-	99.17
10	10.88	14.00	7.44	44.89	20.79	0.83	-	0.93	-	99.76
11	10.5	14.04	7.36	45.14	20.7	0.79	-	0.94	-	99.47
12	11.13	14.02	7.38	45.11	20.78	0.79	-	0.91	-	100.12
13	10.16	14.05	7.38	45.21	20.76	0.80	-	0.89	-	99.25
14	10.38	14.01	7.38	45.42	20.74	0.87	-	0.94	-	99.75
15	10.32	14.06	7.41	45.13	20.62	0.81	-	0.92	-	99.26
16	10.06	14.12	7.41	45.21	20.67	0.68	-	0.91	-	99.06
17	11.06	14.16	7.42	45.71	20.81	0.69	-	0.92	-	100.77
18	10.07	14.28	7.42	45.59	20.88	0.64	-	0.88	-	99.76
19	10.49	14.06	7.38	45.44	20.75	0.81	-	0.96	-	99.88
20	10.75	14.06	7.45	45.16	20.81	0.751	-	0.95	-	99.93
Mean	10.48	14.06	7.40	45.28	20.76	0.77	-	0.92	-	99.66
Std.	0.36	0.07	0.02	0.24	0.08	0.06	-	0.03	-	0.46

252 Table.7: Electron microprobe analyses of sample CRG01

253

No.	B_2O_3	Al_2O_3	MgO	SiO_2	CaO	SO_3	ZnO	CuO	TeO_2	Total
1	15.08	13.42	7.56	42.27	19.89	-	-	-	0.99	99.21
2	15.14	13.35	7.50	42.03	19.80	-	-	-	0.98	98.80
3	15.47	13.44	7.59	41.49	19.86	-	-	-	0.92	98.77
4	15.3	13.33	7.54	41.21	19.83	-	-	-	1.00	98.21
5	15.08	13.41	7.55	41.24	20.07	-	-	-	0.94	98.29
6	15.49	13.33	7.51	42.09	20.03	-	-	-	0.91	99.36
7	15.59	13.24	7.47	41.70	19.86	-	-	-	1.00	98.86
8	15.14	13.33	7.50	41.79	19.85	-	-	-	0.89	98.50
9	15.21	13.29	7.45	41.88	19.88	-	-	-	0.91	98.62
10	15.81	13.22	7.56	41.96	19.72	-	-	-	0.88	99.15
11	15.63	13.22	7.43	42.02	19.94	-	-	-	0.91	99.15
12	15.55	13.30	7.47	41.13	19.88	-	-	-	0.97	98.30
13	15.31	13.37	7.49	41.49	19.95	-	-	-	1.00	98.61
14	15.26	13.33	7.49	41.68	19.79	-	-	-	1.00	98.55
15	15.50	13.43	7.59	42.29	19.84	-	-	-	0.97	99.62
16	15.15	13.44	7.54	41.65	19.80	-	-	-	1.01	98.59
17	15.20	13.37	7.52	41.49	19.90	-	-	-	0.97	98.45
18	16.26	13.39	7.55	41.81	20.02	-	-	-	0.98	100.01
19	15.19	13.25	7.42	41.74	19.87	-	-	-	0.94	98.41
20	15.27	13.36	7.48	42.64	19.93	-	-	-	0.92	99.60
Mean	15.38	13.34	7.51	41.78	19.89	-	-	-	0.95	98.85
Std.	0.28	0.07	0.05	0.38	0.08	-	-	-	0.04	0.49

References

(1) Mysen, B. O.; Virgo, D. Structure and Properties of Silicate Glasses and Melts; Theories and Experiment. In *Advanced Mineralogy*; Marfunin, A. S., Ed.; Springer Berlin Heidelberg, 1994; pp 238–254. DOI: 10.1007/978-3-642-78523-8_14.

(2) Morris, J. D.; Ryan, J. G. Subduction Zone Processes and Implications for Changing Composition of the Upper and Lower Mantle. In *Treatise on Geochemistry*; Elsevier, 2003; pp 451–470. DOI: 10.1016/B0-08-043751-6/02011-9.

(3) Sossi, P. A.; Klemme, S.; O'Neill, H. S.; Berndt, J.; Moynier, F. Evaporation of moderately volatile elements from silicate melts: experiments and theory. *Geochimica et Cosmochimica Acta* **2019**, *260*, 204–231. DOI: 10.1016/j.gca.2019.06.021.

(4) Sossi, P. A.; Moynier, F.; Treilles, R.; Mokhtari, M.; Wang, X.; Siebert, J. An experimentally-determined general formalism for evaporation and isotope fractionation of Cu and Zn from silicate melts between 1300 and 1500 ˚C and 1 bar. *Geochimica et Cosmochimica Acta* **2020**, *288*, 316–340. DOI: 10.1016/j.gca.2020.08.011.

(5) Hashimoto, A. Evaporation metamorphism in the early solar nebula. Evaporation experiments on the melt FeO-MgO-SiO2-CaO-Al2O3 and chemical fractionations of primitive materials. *Geochem. J.* **1983**, *17* (3), 111–145. DOI: 10.2343/geochemj.17.111.

(6) Richter, F. M.; Janney, P. E.; Mendybaev, R. A.; Davis, A. M.; Wadhwa, M. Elemental and isotopic fractionation of Type B CAI-like liquids by evaporation. *Geochimica et Cosmochimica Acta* **2007**, *71* (22), 5544–5564. DOI: 10.1016/j.gca.2007.09.005.

(7) Richter, F. M.; Dauphas, N.; Teng, F.-Z. Non-traditional fractionation of non-traditional isotopes: Evaporation, chemical diffusion and Soret diffusion. *Chemical Geology* **2009**, *258* (1-2), 92–103. DOI: 10.1016/j.chemgeo.2008.06.011.

(8) Wang, J.; Davis, A. M.; Clayton, R. N.; Mayeda, T. K.; Hashimoto, A. Chemical and isotopic fractionation during the evaporation of the FeO-MgO-SiO2-CaO-Al2O3-TiO2 rare earth element melt system. *Geochimica et Cosmochimica Acta* **2001**, *65* (3), 479–494. DOI: 10.1016/S0016-7037(00)00529-9.

(9) Norris, C. A.; Wood, B. J. Earth's volatile contents established by melting and vaporization. *Nature* **2017**, *549* (7673), 507–510. DOI: 10.1038/nature23645.

(10) Renggli, C. J.; Klemme, S. Experimental constraints on metal transport in fumarolic gases. *Journal of Volcanology and Geothermal Research* **2020**, *400*, 106929. DOI: 10.1016/j.jvolgeores.2020.106929.

(11) Jochum, K. P.; Stoll, B.; Herwig, K.; Willbold, M.; Hofmann, A. W.; Amini, M.; Aarburg, S.; Abouchami, W.; Hellebrand, E.; Mocek, B.; Raczek, I.; Stracke, A.; Alard, O.; Bouman, C.; Becker, S.; Dücking, M.; Brätz, H.; Klemd, R.; Bruin, D. de; Canil, D.; Cornell,

D.; Hoog, C.-J. de; Dalpé, C.; Danyushevsky, L.; Eisenhauer, A.; Gao, Y.; Snow, J. E.; Groschopf, N.; Günther, D.; Latkoczy, C.; Guillong, M.; Hauri, E. H.; Höfer, H. E.; Lahaye, Y.; Horz, K.; Jacob, D. E.; Kasemann, S. A.; Kent, A. J. R.; Ludwig, T.; Zack, T.; Mason, P. R. D.; Meixner, A.; Rosner, M.; Misawa, K.; Nash, B. P.; Pfänder, J.; Premo, W. R.; Sun, W. D.; Tiepolo, M.; Vannucci, R.; Vennemann, T.; Wayne, D.; Woodhead, J. D. MPI-DING reference glasses for in situ microanalysis: New reference values for element concentrations and isotope ratios. *Geochem. Geophys. Geosyst.* **2006**, *7* (2), n/a-n/a. DOI: 10.1029/2005GC001060.

(12) Klemme, S.; Prowatke, S.; Münker, C.; Magee, C. W.; Lahaye, Y.; Zack, T.; Kasemann, S. A.; Cabato, E. J. A.; Kaeser, B. Synthesis and Preliminary Characterisation of New Silicate, Phosphate and Titanite Reference Glasses. *Geostand Geoanalyt Res* **2008**, *32* (1), 39–54. DOI: 10.1111/j.1751-908X.2008.00873.x.

(13) Holloway, J.; Wood, B. J. *Simulating the Earth: Experimental Geochemistry*; Unwin Hyman Inc., 1988.

(14) Hinton, R. W. NIST SRM 610, 611 and SRM 612, 613 Multi-Element Glasses: Constraints from Element Abundance Ratios Measured by Microprobe Techniques. *Geostandards and Geoanalytical Research* **1999**, *23* (2), 197–207. DOI: 10.1111/j.1751-908X.1999.tb00574.x.

(15) Eggins, S. M.; Shelley, J. M. G. Compositional Heterogeneity in NIST SRM 610-617 Glasses. *Geostandards and Geoanalytical Research* **2002**, *26* (3), 269–286. DOI: 10.1111/j.1751-908X.2002.tb00634.x.

(16) Morizet, Y.; Ory, S.; Di Carlo, I.; Scaillet, B.; Echegut, P. The effect of sulphur on the glass transition temperature in anorthite–diopside eutectic glasses. *Chemical Geology* **2015**, *416*, 11–18. DOI: 10.1016/j.chemgeo.2015.10.010.

(17) Larre, C.; Morizet, Y.; Bézos, A.; Guivel, C.; La, C.; Mangold, N. Particular H 2 O dissolution mechanism in iron-rich melt: Application to martian basaltic melt genesis. *J Raman Spectrosc* **2020**, *51* (3), 493–507. DOI: 10.1002/jrs.5787.

(18) Bowen, N. L. The crystallization of haplobasaltic, haplodioritic, and related magmas. *American Journal of Science* **1915**, *s4-40* (236), 161–185. DOI: 10.2475/ajs.s4-40.236.161.

(19) Huber, C.; Jahromy, S. S.; Birkelbach, F.; Weber, J.; Jordan, C.; Schreiner, M.; Harasek, M.; Winter, F. The multistep decomposition of boric acid. *Energy Sci Eng* **2020**, *8* (5), 1650–1666. DOI: 10.1002/ese3.622.

(20) Anzures, B. A.; Parman, S. W.; Milliken, R. E.; Namur, O.; Cartier, C.; Wang, S. Effect of sulfur speciation on chemical and physical properties of very reduced mercurian melts. *Geochimica et Cosmochimica Acta* **2020**, *286*, 1–18. DOI: 10.1016/j.gca.2020.07.024.

For Table of Contents Only